A Low Complexity Channel Emulator for Underwater Acoustic Communications

Chenyang Zhang, Yixuan Xie, Deepak Mishra, Tom Pacino, Jeffrey Shao, Bo Li, Jinhong Yuan
University of New South Wales Sydney, Australia
{chenyang.zhang1, yixuan.xie, d.mishra, t.pacino, jeffrey.shao, bo.li7, j.yuan}@unsw.edu.au
Peng Chen, Yue Rong
Curtin University Perth, Australia {y.rong, peng.chen}@curtin.edu.au

***Abstract*—This paper presents a low-complexity channel emulator for underwater acoustic communications. The proposed emulator utilizes Bellhop's underwater acoustic toolbox to calculate the channel response at the beginning and end of each stationary time interval. It also takes into account the motion of the transmitter and receiver to compute the Doppler factor. It applies a low-complexity resampling method for each path to generate the channel output signals during each stationary interval. This emulator assumes that the channel is doubly selective. To verify the emulator, a software-defined radio platform is used for implementation. The numerical results demonstrate that the proposed emulator achieves higher accuracy and much lower complexity than the existing underwater channel emulator based on Waymark.**

***Index Terms*—Underwater Acoustic Communications, Doubly Selective Channel, Channel Emulator, Software Defined Radio**

I. Introduction

Research on underwater acoustic (UWA) communication is rapidly developing due to its crucial role in various applications, such as underwater exploration, marine biology, and oceanography. However, underwater environments present significant challenges that differ from conventional wireless communication systems over the air. Distinctive properties such as temperature, salinity, pressure, noise, and water currents can cause a complex and unpredictable channel, which can significantly affect communication performance [1]. Due to these challenges posed by underwater environments, effective communications require unique and advanced solutions that can uphold high-speed and dependable communication.

A. State of the Art

Three leading technologies are available for underwater wireless communications: acoustic waves, electromagnetic (EM) waves that use radio frequencies (RF), and optical waves. Each technology has its advantages and drawbacks, which make it suitable for different scenarios [2]. EM waves in the radio frequency band are commonly used for communication purposes. Optical wave communications present an alternative technology, providing higher data rates than EM wave communications. However, both RF and optical waves have limited transmission ranges due to high environmental distortions in water. RF waves have high attenuation, while optical waves are suffered from high water absorption and floating particle scattering. Acoustic waves are the most widely employed technique in long-distance underwater environments [2]. Compared to EM waves, acoustic waves have low attenuation in water, can cover longer distances and have more significant application potential. However, the reflection and refraction of waves between the surface and seafloor affect signal propagation, which leads to a significant delay spread during communications. Besides, the Doppler effects of each path cannot be ignored for a UWA wave. For each path, the delay and the Doppler effects are unique [3]. Thus, the UWA channel can be considered as a doubly-selective channel [4]. These factors present significant challenges to the communication system capability [5].

Testing and validating new UWA systems designed in natural environments is time-consuming and expensive. Several efforts have been devoted to model UWA signal transmission. A toolbox, Bellhop, can simulate the path traces and get the parameters of each path based on provided environment and test requirements [6]. The delay and amplitude of each path can be calculated from Bellhop. When the transmitter or the receiver moves, the signal is influenced by the Doppler effect. Theoretically, it is possible to compute amplitudes and delays at each sampling time step using ray traces of the location. However, employing Bellhop directly for simulation at each sampling time proves highly computationally expensive, making it impractical in reality [7].

Some researchers use frequency shifts to emulate the channel with the Doppler effect. Vlastaras et al. implemented a two-ray channel for testing IEEE 802.11p [8]. Ghiaasi et al. used a tapped delay line (TDL) model with a clustering algorithm to reduce the number of propagation paths that need to be emulated [9]. Hofer et al. build an emulator using a low-complexity reduced-rank subspace model [10]. Carlos et al. proposed a non-wide-sense stationary uncorrelated scattering (non-WSSUS) mobile-to-mobile Rayleigh fading channel based on statistical geometry modelling, which analyzes the channel based on the movement of the transmitter and receiver. This model provides the time-delay or time-frequency domain response [11]. Ruiz-García et al. separated the time and frequency into discrete components and developed the non-WSSUS channel emulator [12].

Another approach for the UWA channel model is to use the time-variant channel model. Liu et al. proposed the Waymark channel model for UWA communications [4], which generates

979-8-218-14218-6 ©2023 MTS

the channel response at the beginning of each stationary time and uses local-spline interpolation to link up these channel responses between different stationary times. Henson et al. tested shallow water experiments following the waymark method, which showed similar results to the VirTEX model [13].

B. Motivation and Contribution

The existing literature suggests that there is a need for new underwater acoustic communication systems that can characterize the impact of Doppler scaling doubly selective channels.

The summary of our novel contributions to this work is given as follows:

- Develop a novel channel emulator framework for UWA communications. This framework models the Doppler scaling through a low-complexity resampling method, which avoids errors caused by considering Doppler scaling as a frequency shift and saves on calculations.
- Analyse the received signal and characterize the impact of Doppler scaling doubly selective channels.
- Implement the emulator using the Universal Software Radio Peripheral (USRP) software-defined radios (SDR) kit that can enable easy testing usage.
- Validate and compare the proposed method with the existing benchmarks. Besides, we analyze the influence of the Doppler effect on OFDM signals.

II. Underwater Acoustic Channel

Several environmental factors influence UWA channels and have different features in different scenarios. The channels are characterized by high attenuation and time-varying multipath propagation. The UWA channel is a linear time-variant channel and can be analyzed based on separate paths. For a given input signal $s(t)$, the channel output $r(t)$ is given by

$$r(t) = \sum_{i=1}^{N} h_i(t) s\left(\alpha_i \cdot (t - \tau_i)\right) + w(t), \tag{1}$$

where N is the number of paths, $w(t)$ is the surrounding noise, $h_i(t)$ is the channel coefficient of the i-th path, α_i is the Doppler factor and τ_i is the initial delay, which will be explained later.

The Doppler effect arises due to the relative movement of the source and receiver. This relative motion can cause time-varying delays and signal compression or expansion in the time domain. In [4], a common definition of the linear time-varying channel is

$$r(t) = \int_{-\infty}^{\infty} \kappa(t, \tau) s(t - \tau) \mathrm{d}\tau, \tag{2}$$

where $\kappa(t, \tau)$ is the time-varying impulse response. For simple illustration purposes, let us first consider only one path. Thus, there will be one impulse response for a given time t due to the i-th path. The time-varying impulse response is $\kappa(t, \tau) = h_i(t)\delta(t - \tau_i(t))$, where $\tau_i(t)$ is the delay of the i-th path. It means the delay-varying property causes the channel to be time-variant. Thus, in the rest of the section, the relationship between delay and the Doppler effect is analyzed in a one-path. Fig. 1 illustrates a single-path channel model. The propagation distance between the transmitter and receiver is denoted by l_i, which includes the lengths of the transmitter and receiver movements as well as the sound transmission distance. Let $v_s(t)$ and $v_r(t)$ be the transmitter and receiver velocities and c is the speed of sound, respectively. The total path length l_i for the i-th path is given by:

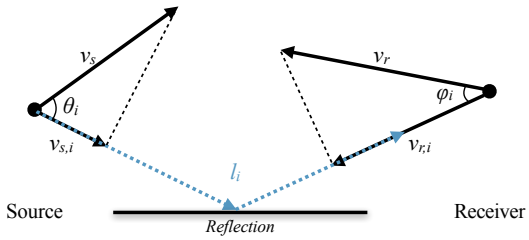

Fig. 1. One route example

$$l_i = \int_0^{t_{r,i}} v_{r,i}(t)\mathrm{d}t + \int_0^{t_s} v_{s,i}(t)\mathrm{d}t + c\tau_i(t). \tag{3}$$

Here, $v_{s,i}(t) = v_s(t)\cos\theta_i(t)$ and $v_{r,i}(t) = v_r(t)\cos\varphi_i(t)$ denote the radial velocities of the transmitter and receiver, respectively, along the propagation direction. The angles $\theta_i(t)$ and $\varphi_i(t)$ are the angles between the propagation direction and the transmitter or receiver, respectively. The time difference between the receiver and transmitter is given by $\tau_i(t) = t_{r,i} - t_s$, where t_s and $t_{r,i}$ denotes the transmission time and the receiver time of the i-th path.

In a scenario where the velocities and propagation angles of the transmitter and receiver remain relatively constant over a period of time. This is referred to as the stationary time, and the channel can be considered stable and hence changing linearly. In this case, the radial velocities of the transmitter and the receiver can be considered as constant values $v_{s,i}$ and $v_{r,i}$, and the relationship of the transmitted time and received time, as deduced from (3), can be written as

$$t_{r,i} = \frac{(c - v_{s,i})t_s + l_i}{c + v_{r,i}}. \tag{4}$$

The relationship between transmitted signal $s(t)$ and received signal of the i-th path $r_i(t)$ is:

$$r_i(t) = h_i(t) s\left(\frac{c + v_{r,i}}{c - v_{s,i}}(t - \tau_i)\right), \tag{5}$$

where $\tau_i = \frac{l_i}{c + v_{r,i}}$ is the initial delay of the i-th path. Thus, the underlying Doppler factor for the i-th path can be defined as

$$\alpha_i \triangleq \frac{c + v_{r,i}}{c - v_{s,i}}. \tag{6}$$

For each path, the signal is compressed or dilated due to the Doppler effect. The received signal is the summation of each path and additional noise, shown in (1).

In the frequency domain, the expression for $R_i(f)$, the received signal at frequency f, can be derived as:

$$R_i(f) = H_i(f) * S\left(\frac{f}{\alpha_i}\right) e^{-j2\pi f \tau_i}, \tag{7}$$

where $S(f)$ and $H_i(f)$ represent the Fourier transform of the transmitted signal $s(t)$ and the channel response $h_i(t)$. When the signal bandwidth is narrow enough, such that $B \ll f_c$, where f_c is the carrier frequency, the Doppler effect can be treated as a frequency shift [14]. If the bandwidth does not satisfy this requirement, the signal is applied with not only a frequency shift but a bandwidth compression or dilation. It is known as the effect of Doppler scaling.

The level of the Doppler effect in each path is decided by the radial velocity, which is dependent on both the velocity and the angles between the propagation path and movement directions. As a result, each path has its own delay and Doppler factor. This means that the underwater acoustic channel can be represented as a doubly selective channel.

In the UWA scenario, the wave propagation speed is approximately 1500 m/s, which can result in a more significant Doppler effect compared to the speed of electromagnetic waves over the air. For instance, when the receiver is moving at a speed of 15 m/s toward the transmitter, the Doppler factor in UWA is approximately $\alpha = 1.01$, whereas it is only $\alpha = 1.00000005$ in traditional wireless communications. Consider a typical UWA OFDM system with bandwidth 4kHz and 512 subcarriers. The amount of frequency change due to α is approximately 40Hz. This is almost 5 times the subcarrier spacing $\Delta f = \frac{4000}{512} \approx 7.8$Hz. However, in traditional wireless communications with 20 MHz bandwidth and 1024 carriers, the bandwidth change is 1 Hz, and it is a very tiny 5×10^{-5} fraction of the subcarrier spacing. Despite the larger bandwidth in conventional wireless systems, the scaling impact of the Doppler effect is more pronounced in UWA communications, while for wireless communications, the Doppler shift is the main effect.

III. Emulator Architecture

Now we briefly explain the basic idea behind the resampling-based channel emulation method.

In hardware implementations, discrete-time signals are processed. Let the sampling duration for the transmit signal be T_s. The transmit signal is expressed by $s[n] = s(nT_s)$. The received signals are sampled at the intervals of T_r. Using (1), the discrete received signal can be represented as:

$$r[n] = \sum_{i=1}^{N} h_i[n] s\big(\alpha_i \cdot (nT_r - \tau_i)\big) + w[n]. \tag{8}$$

This equation shows that the signal is resampled through a multi-Doppler scaling channel. The sampling interval changes from T_s to $\alpha_i T_r$ to apply the Doppler scaling for the i-th path. To emulate the entire multipath system, each path can be simulated by adding delay, resampling and applying channel coefficient, and then the signals of all paths are superimposed to generate the received signal.

A. Resampling Based Channel Emulation Method

In order to create a more realistic representation, the emulator takes into account varying Doppler factors during each frame transmission. To handle this, resampling processing is done at each stationary time interval. This involves generating ray parameters for each path separately during each stationary interval and then combining the outputs from all intervals to create the final channel emulator output.

Let us consider the stationary time as T, the index of the stationary time as j, and that there are $P = \frac{T}{T_r}$ samples in one stationary time. The Doppler factors, as calculated by the difference between the initial delay of two stationary intervals, can be defined as:

$$\alpha_i(j) = \frac{T}{\tau_i(jT+T) - \tau_i(jT) + T}. \tag{9}$$

The index of the sample in one stationary time is n_T, the channel coefficient is generated by linear interpolation

$$\hat{h}_i(n) = \frac{P - n_T}{P} h_i(jT) + \frac{n_T}{P} h_i(jT+T), \tag{10}$$

which follows $n = (j-1)P + n_T, 0 \le n_T < P$. If there is a total of L intervals simulated, the received signal by resampling method can be expressed as:

$$r[n] = \sum_{i=1}^{N} \sum_{k=0}^{L} \hat{h}_i\big(\beta_{n,k} + kT\big) s\big(\beta_{n,k} + kT\big) \Pi_T\big(\beta_{n,k}\big) + w[n], \tag{11}$$

where k is the index of each stationary time slot and

$$\beta_{n,k} = \alpha_i(k)\big(nT_r - \tau_i(kT) - kT\big), \tag{12}$$

which illustrates the delay and Doppler effect. Each stationary time is applied by a window function $\Pi_T(t) = 1$ for $0 < t < T$ and $\Pi_T(t) = 0$ elsewhere.

Fig. 2 shows the processing of the resampling method for the i-th path. The emulator adjusts the time intervals of each

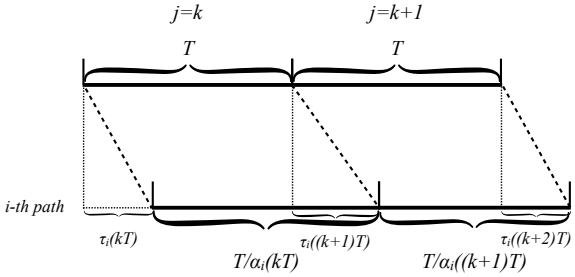

Fig. 2. Resampling Implement

sequence based on the channel response during stationary periods. It applies the channel response separately for each path and uses resampling to make adjustments. Ultimately, the emulator outputs are combined by concatenating the results from all stationary intervals.

The resampling technique does not require the channel impulse response for every sample. Instead, it applies the

channel to the input signal based on the delay time of the start and end of each stationary period. The emulator concentrates on the impact of motion on the channel, while disregarding the surface alterations caused by waves and the changes in water flow.

B. Emulator Tools

To generate ray parameters, this emulator makes use of a toolbox called Bellhop and performs signal processing using LabVIEW. The Ocean Acoustics Library (OALIB) offers an acoustic toolbox, Bellhop, which is a beam-tracing model used in the ocean environment [6]. The Bellhop model requires input such as environmental data, simulation specifications, and the positions of the transmitter and receiver. The movement calculates the position during a specific time and Bellhop generates rays connecting the source and receiver using the 'Eigenray' method. The output from this method includes ray parameters such as delay, channel coefficient, angles, and reflection times for each path.

We run Bellhop at the beginning of each stationary time and get the ray parameters as a channel set. Then LabVIEW can use this set to distinguish paths, calculate the Doppler factors and apply Doppler and delay to the input signal.

We choose USRP N210 as the hardware platform, which can achieve 100 M Sample/s analogue to digital converter (ADC) rate and 400 M Sample/s digital to analogue converter (DAC) rate. A pair of low-frequency front-ends, LFTX/LFRX daughterboards, are used for transmitting and receiving the signal at a frequency range of $0 - 30$ MHz.

C. System Overview Flow Chart

Fig. 3 shows the system diagram of the designed channel emulator. The input baseband signal is upconverted to the passband. The transmitter and receiver movement is used to generate the propagation environment files for each stationary time. Bellhop generates the ray parameters, which contribute to the channel set. Emulator distinguishes each path and computes the Doppler factors for each stationary time using (9). Then the emulator applies the channel characteristics by adding delay and resampling for each path and adding the responses from all paths together based on (11). Finally, the processed signal is sent to the hardware and transmitted through the transducer. It is commonly known that the signal goes through hardware, DAC, and upconversion and then is transmitted via transducers. However, in the underwater acoustic scenario, the carrier frequency is much lower than in the traditional wireless case, which means we can process the digital passband signal. Thus, the up-conversion is employed only in software before DAC.

IV. Performance Evaluation

A. Simulation Parameters

To evaluate the emulator performance, we generate an underwater acoustic environment with the transmitter and the receiver at a depth of 50m and 70m. The depth of the sea is 200m and the range between transmitter and receiver is 1 km. We consider an orthogonal frequency division multiplexing (OFDM) signal using Quadrature Phase Shift Keying (QPSK) as the source, which can be defined as

$$x(t) = \mathbb{R}\left(\sum_{k=1}^{K} A(k) e^{j2\pi(f_c + (k-\frac{K}{2})\Delta f)t}\right), \qquad (13)$$

where $f_c = 12$ kHz is the carrier frequency, $K = 64$ is the total number of subcarriers, k stands for the index of each subcarrier, $A(k)$ is the QPSK symbol at each subcarrier, $\Delta f = 62.5$ Hz is the subcarrier spacing for bandwidth of 4 kHz and '$\mathbb{R}$' denotes the real part of the signal. Here, we first generate the QPSK symbols $A(k), \forall k = \{1, 2, ..., K\}$ and then apply inverse Fast Fourier Transform (IFFT) to get the OFDM sequence before passing it to the filter and the up-conversion component in LabVIEW.

B. Validation Results

For illustration purposes, Fig. 4 shows the frequency spectrum of a signal before and after Doppler scaling. From Fig. 4(a) $\alpha = 0.9$, the receiver is moving away from the transmitter at a speed of 150 m/s. Therefore, the bandwidth of the spectrum after scaling gets compressed, and the centre frequency shifts to 10.8 kHz from 12 kHz. In contrast, when the receiver is moving closer to the transmitter as represented in Fig. 4(b) $\alpha = 1.1$. The frequency spectrum dilates after Doppler scaling and the center frequency correctly shifts to 13.2 kHz. These results validate that our proposed resampling method can be used to apply the Doppler scaling to the input OFDM signal sequence. Note that the extremely high moving speed and Doppler factor in Fig. 4 are only for illustration. In reality, the Doppler factor is much smaller.

In order to ensure the accuracy of our emulator design, we have considered three different approaches. The first approach is called the Bellhop method, where Bellhop is run for each sample time. Additionally, we have also utilized the Waymark method [13] and our own resampling method.

The stationary time is determined by the velocities of the transmitter and receivers, and is chosen based on observation. A shorter stationary time is needed for faster movement speeds. Fig. 5 demonstrates that channel responses of each path vary with a velocity of 40 m/s within a stationary time. Fig. 6 shows channel responses over several stationary times for a longer duration. These figures illustrate that both delays and amplitudes of all the paths change linearly within a duration of 0.05 s, though the delay changes are not obvious compared to the amplitude. Thus, we have chosen this duration as the stationary time.

In Fig. 7, we can see the received signal produced by different channel emulation methods. The magenta line represents the output signal of the resample method, the yellow line is the output signal of the Waymark method, and the blue line represents the output signal of the frequent Bellhop. It is evident that the signal is almost identical, but the resampling method takes significantly less time than the frequent Bellhop method. Fig. 7(a) shows the input signal as a sine wave with a frequency of 4 kHz, while the input sequence for Fig. 7(b)

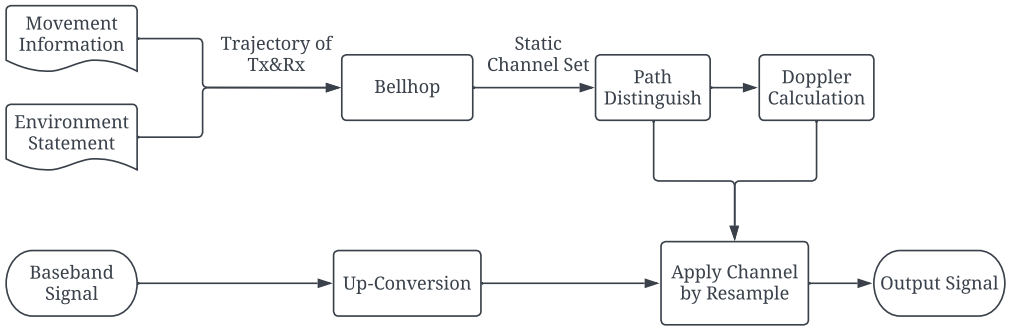

Fig. 3. Emulator Block Diagram

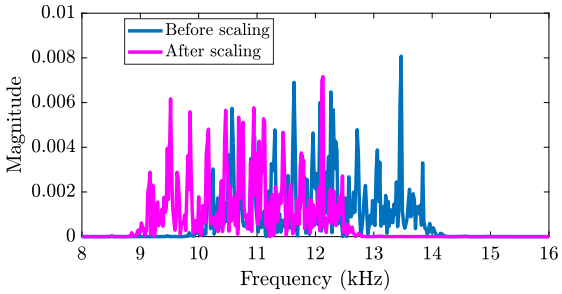

(a) $\alpha = 0.9$

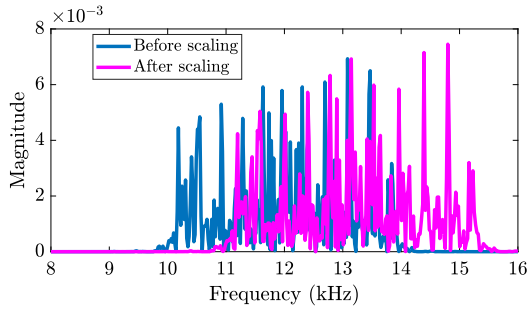

(b) $\alpha = 1.1$

Fig. 4. Frequency spectrum of $x(t)$ before and after Doppler Scaling

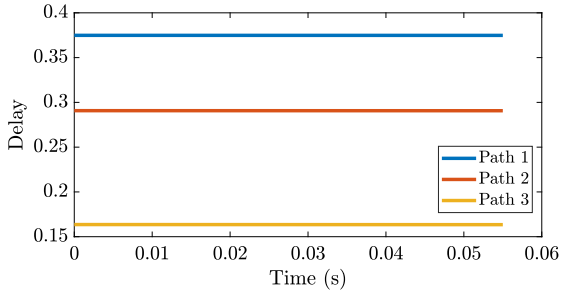

(a) Delay

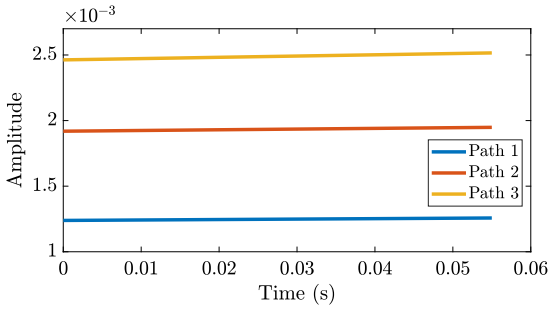

(b) Amplitude

Fig. 5. Channel Response during A Stationary Time

is an OFDM signal with a bandwidth of 4 kHz. All methods display similar results, indicating that they apply comparable Doppler scaling to the input signal. However, when the input signal is an OFDM sequence signal, the resampling method is more similar to the frequent Bellhop result compared to the Waymark method. The mean squared error (MSE) is used to assess the similarity between signals, which is calculated by the equation: $MSE = \mathbb{E}\Big(\big(r_{Bellhop}[n] - \hat{r}[n]\big)^2\Big)$. Here $\hat{r}[n]$ can be $r_{Waymark}[n]$ and $r_{Resample}[n]$. We consider frequent Bellhop results as a reference and calculate the MSE of the Waymark method and our resampling method. Fig. 8 illustrates the variety of MSE over time. The MSE for the Waymark method is represented by the magenta line, while the blue line shows the MSE for the resampling method. Throughout the processing duration, the MSE for the Waymark model remains consistently higher than that of the resampling method. This indicates that the resampling method is more accurate than Waymark.

For the OFDM system, Doppler scaling affects the performance significantly. The characteristics of the channel-applied OFDM signal are analyzed. The received passband signal $r_p(t)$ of one OFDM frame is given by, based on (5),

$$r_p(t) = \sum_{i}^{N} \mathbb{R}\left(h_i \sum_{k=1}^{K} A(k) e^{j2\pi(f_c + (k-\frac{K}{2})\Delta f)\alpha_i t} \right) + w(t). \quad (14)$$

After the down-conversion and equalization, the delay of each path is removed and the processed baseband signal $r_b(t)$ is

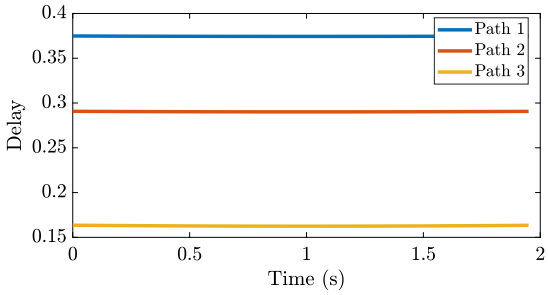

(a) Delay

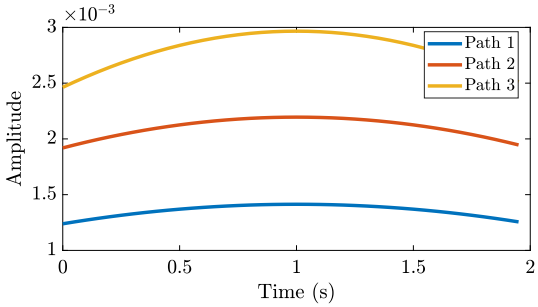

(b) Amplitude

Fig. 6. Channel Response over a Stationary Time

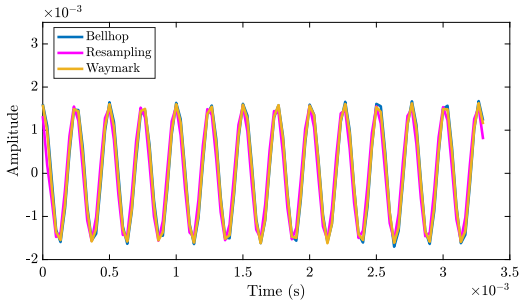

(a) Sine Wave Signal

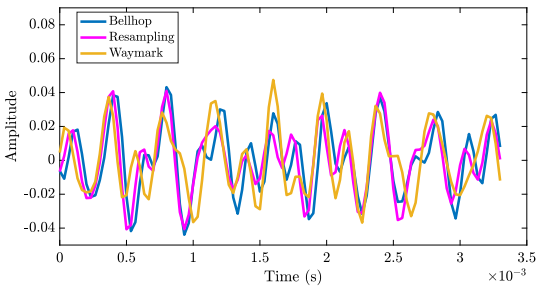

(b) OFDM Signal

Fig. 7. Resample method compare to the Frequent Bellhop

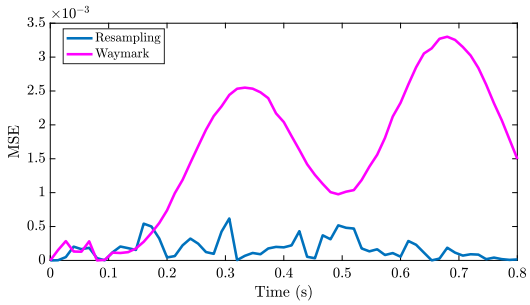

(a) Sine Wave Signal

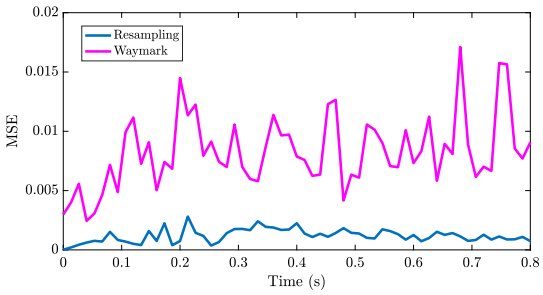

(b) OFDM Signal

Fig. 8. MSE of the Waymark method and Resampling method

written as:

$$r_b(t) = \sum_{i}^{N}\left(\sum_{k=1}^{K} A(k)e^{j2\pi(k-\frac{K}{2})\Delta f t}e^{j2\pi(k-\frac{K}{2})\Delta f(\alpha_i-1)t}\right) e^{j2\pi(\alpha_i-1)f_c t} + w(t), \tag{15}$$

in which, $e^{j2\pi(\alpha_i-1)f_c t}$ shows the effect of the Doppler shift for the carrier frequency, meaning the rotation of the constellation, causing a phase error. And the $e^{j2\pi(k-\frac{K}{2})\Delta f(\alpha_i-1)t}$ is the additional frequency shift, which is different for each subcarrier. For the edge subcarriers, the extra frequency shift is large while it is small for subcarriers close to the center. Thus, each point on the constellation is spreading to an arc.

Here we test the OFDM signal applied with our resampling method channel with different receiver velocities, 0.1, 0.2 and 0.3 m/s, and the corresponding Doppler factor $\alpha = 1.000016, 1.000032, 1.000048$. After the OFDM demodulation, the constellations of received signals are shown in Fig. 9. In this diagram, there are three constellations that move at different speeds. The blue dots represent the demodulated samples. It's easy to see that when the velocity is higher, the Doppler effect is stronger.

Each set of points represents a QPSK symbol that was sent. In each group, the center dot rotates more noticeably, while the other dots spread out in an arc shape over a longer distance.

C. Complexity Analysis

The complexity of the resampling method depends on the length of the sequence and the number of paths in the channel.

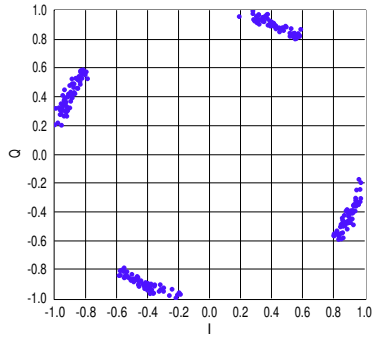

(a) $v_r = 0.1m/s$

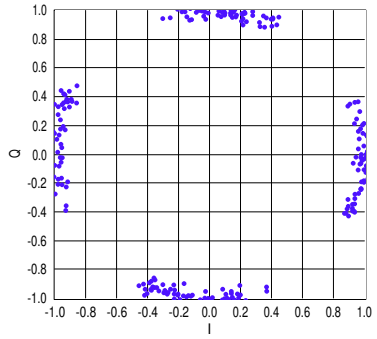

(b) $v_r = 0.2m/s$

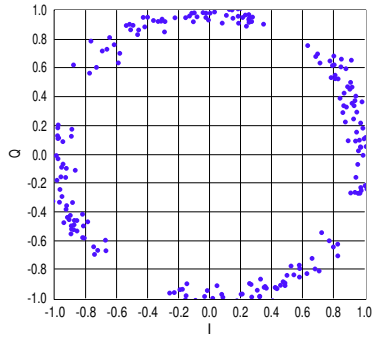

(c) $v_r = 0.3m/s$

Fig. 9. Constellation of the OFDM signal with Different Doppler Scaling.

Here, the complexity of Bellhop is assumed as $\mathcal{K}$ and there are average N_{path} paths during the processing and the number of the input samples is N_s. For the frequent Bellhop method, the complexity is $\mathcal{O}((\mathcal{K} + N_{path})N_s)$. The resampling function depends on the stationary time. The complexity is $\mathcal{O}((\frac{\mathcal{K}}{P} + N_{path})N_s)$.

In contrast, the Waymark method involves multiple matrix multiplications, leading to a high complexity. The complexity depends on the matrix size and calculation time, which increase with wider bandwidth or reduced stationary time length. Additionally, the required Fast Fourier Transform impacts the complexity, which is influenced by the sampling frequency. The support of the cubic B-spline in the Waymark method is $N_B = 4$ [4] and it considers the previous and latter two channel response. Assuming the sampling frequency is F_s, each stationary time includes matrix multiplications for delay compensation with $P \times N_B \times (N_B + 2)$ operations, another $P \times N_B \times (N_B + 2)$ operations for Delay spline interpolation, and $P \times F_s \times N_B^2$ operations for calculate the output signal. Thus, the total complexity is about $\mathcal{O}((\frac{\mathcal{K}}{P} + F_s \times N_B^2))N_s)$.

TABLE I
TIME SPENDING COMPARISION

Time Cost (s)	Default	Far	Deep	Longer Signal	Shorter Stationary
Bellhop	10615	10654	11075	21572	10615
Resampling	57	71	51	109	69
Waymark	156	193	150	217	203

In Table I, you can see the time difference when running the emulator for various UWA environments. The resampling method and Waymark method both run quickly during signal processing and the Bellhop step. The complexity is not significantly affected by changes in the environment. However, the calculation time increases with longer sequences or shorter stationary times, resulting in more stationary intervals.

V. CONCLUDING REMARKS AND FUTURE DIRECTIONS

In this paper, we explored the processing of the Doppler effect in both the time and frequency domains, revealing how the Doppler scaling channel works and how it compresses or dilates signals. With this knowledge, we developed a new emulator that utilizes the Bellhop toolbox to simulate the underwater acoustic channel. By using the resample method, we can reduce computation costs while maintaining high accuracy. This emulator is a valuable tool for testing UWA communication systems and saves time during the testing process. Moving forward, we plan to consider the impact of ocean surface waves and flow variations to make the emulator even more realistic. Overall, this work contributes to the advancement of research in underwater acoustic communication by providing novel insights into the impact of Doppler scaling while modelling UWA channels.

REFERENCES

[1] M. Lanzagorta, "Underwater communications," *Synthesis lectures on communications*, vol. 5, no. 2, pp. 1–129, 2012.
[2] A. V. Gadagkar and B. R. Chandavarkar, "A comprehensive review on wireless technologies and their issues with underwater communications," in *Proc. 12th Int. Conf. on Comput. Commun. Netw. Tech. (ICCCNT)*, Jul. 2021, pp. 1–6.
[3] Y. V. Zakharov and V. Kodanev, "Multipath-Doppler diversity of OFDM signals in an underwater acoustic channel," in *Proc. IEEE Int. Conf. Acoust. Speech Signal Process.*, Jun. 2000, vol. 5, pp. 2941–2944.
[4] C. Liu, Y. V. Zakharov, and T. Chen, "Doubly selective underwater acoustic channel model for a moving transmitter/receiver," *IEEE Trans. Veh. Technol.*, vol. 61, no. 3, pp. 938–950, Mar. 2012.
[5] X. Li and D. Zhao, "Capacity research in cluster-based underwater wireless sensor networks based on stochastic geometry," *China Commun.*, vol. 14, no. 6, pp. 80–87, Jun. 2017.
[6] M. B. Porter, *Acoustics Toolbox*, https://oalib-acoustics.org/models-and-software/acoustics-toolbox.
[7] M. Siderius and M.B. Porter, "Modeling broadband ocean acoustic transmissions with time-varying sea surfaces," in *J. Acoust. Soc. Amer.*, vol. 124, no. 1, pp. 137-150, Jul. 2008.
[8] D. Vlastaras, S. Malkowsky, and F. Tufvesson, "Stress test of vehicular communication transceivers using software defined radio," in *Proc. IEEE Vehi. Tech. Conf.*, vol. 41, no. 2, May 2015, pp. 1–4.

[9] G. Ghiaasi, M. Ashury, D. Vlastaras, M. Hofer, Z. Xu, and T. Zemen, "Real-time vehicular channel emulator for future conformance tests of wireless ITS modems," in *Proc. IEEE EuCAP*, Apr. 2016, pp. 1–5.
[10] M. Hofer, Z. Xu, and T. Zemen, "Real-time channel emulation of a geometry-based stochastic channel model on a SDR platform," in *IEEE 18th Int. Workshop on Signal Process. Adv. Wireless Commun.*, Jul. 2017, pp. 1–5.
[11] C. A. Gutiérrez, J. T. Gutiérrez-Mena, J. M. Luna-Rivera, D. U. Campos-Delgado, R. Velázquez, and M. Pätzold, "Geometry-based statistical modeling of non-WSSUS mobile-to-mobile rayleigh fading channels," *IEEE Trans. Vehi. Techn.*, vol. 67, no. 1, pp. 362–377, Jan. 2018.
[12] Á. E. Ruiz-García, C. A. Gutierrez, J. Vázquez-Castillo, and J. Cortez, "SDR-based channel emulator for vehicular communications," in*Proc.COLCOM'19*, Jun. 2019, pp. 1–6.
[13] B. Henson, J. Li, Y. V. Zakharov, and C. Liu, "Waymark baseband underwater acoustic propagation model," in *Proc. IEEE UComms*, Sep. 2014, pp. 1–5.
[14] G. Matz and F. Hlawatsch, "Chapter 1 - fundamentals of time-varying communication channels," in *Wireless Communications Over Rapidly Time-Varying Channels*, F. Hlawatsch and G. Matz, Eds. Oxford: Academic Press, 2011, pp. 1–63.